THE COMPUTATION OF THE AERODYNAMIC BEHAVIOR OF NON-CONVENTIONAL ROTOR TIP CONFIGURATIONS

Final Report for the Period

July 1, 1995 - August 31, 1995

Attn: Dr. Francis X. Caradonna
U.S. Army Aeroflightdynamics Directorate
Mail Stop 215-1
NASA Ames Research Center
Moffett Field, CA 94035

Prepared by

Lakshmi N. Sankar and Nathan Hariharan
School of Aerospace Engineering
Georgia Institute of Technology, Atlanta, GA 30332-0150

November 1995

INTRODUCTION

This research project is aimed at studying the tip vortices generated by a two bladed rotors with an anhydral tip, in hover. An issue to be examined was whether the anhydral shape increases the spacing between the rotor disk and the tip vortex geometry, compared to a straight tip rotor. Such an increase in the spacing is expected to lead to weaker blade vortex interactions, lower vibratory loads and lower BVI noise.

RESEARCH PERSONNEL

The calculations reported here were done by Mr. Nathan Hariharan, a graduate student at Georgia Tech during a one month visit to NASA Ames Research Center. Dr. Francis X. Caradonna of the U. S. Army Aeroflightdynamics Directorate (AFDD) was the technical monitor, and directed this research. Dr. Ramachandran of the U. S. Army AFDD assisted Mr. Hariharan in this effort, and provided numerical solutions for comparison. Dr. L. N. Sankar, was the principal investigator of this effort and assisted Mr. Hariharan in the flow solver development, grid generation effort and in the interpretation of the computed results.

COMPUTER CODES USED

A 3-D unsteady compressible Navier-Stokes solver GT-ENO developed at Georgia tech by the researchers was used in this study. This solver integrates the unsteady compressible Navier-Stokes equations in time using a second order accurate, iterative implicit scheme. The equations are solved in an integral form using a finite volume scheme. The mass, momentum and energy fluxes at the cell faces were computed using a fifth order accurate, non-oscillatory interpolation scheme. Numerical viscosity was built into this flux evaluation using the Roe scheme. All the calculations were done in an inertial frame. A body-fitted coordinate system attached to the rotor was used. This flow solver has been extensively validated for isolated rotor configurations, in the Ph. D. dissertation of Hariharan [1]. Calculations for the anhydral rotor and the straight tip rotor were done in parallel by Ramachandran using the well known HELIX code [2, 3].

RESULTS AND DISCUSSION

Two blade configurations - an anhydral geometry, and a straight tip rotor- were considered. Except for the tip geometry variation, these two configurations were nearly identical facilitating one-to-one comparison between straight and anhydral rotors.

Figure 1 shows the blade planform, the surface grid over the anhydral tip, and the body-fitted grid for the anhydral geometry. For the two-bladed configuration operating in hover considered here, it is sufficient to solve the flow over a single blade, with periodic boundary conditions at the upstream and downstream boundaries.

Figure 2 shows the body fitted grid at a single radial location, and at a single chordwise location. It is seen that the grid is nearly orthogonal to the body surface. This is essential to stable, accurate solutions. It is also seen that the grid lines are clustered only near the blade tip. Elsewhere, the grid lines are sparsely spaced.

Figure 3 shows the computed surface pressure distributions for the straight rotor for a subsonic tip Mach number. Good agreement between the present simulation and the HELIX code are observed in the tip region. the fact that two widely different formulations in use within the GT-ENO and the HELIX code give nearly identical result increases our confidence in the ability of these codes to model details of the tip flow phenomena.

At the inboard stations, the GT-ENO code has very few points, and tends to overpredict the lift and drag as shown in figure 4. The GT-ENO simulation is computationally costly, and had to be stopped after several thousand time steps, when the flow field near the tip has stopped changing. The wake had not fully evolved when the calculations were stopped. This leads to an underprediction of the inflow and an overprediction of the lift. Near the tip, the peak value of C_l as well as the variation are in good agreement with HELIX.

Figure 5 shows the surface pressure distribution for the anhydral tip case. As in the case of the straight tip rotor, agreement with the HELIX code in the immediate vicinity of the tip is excellent.

Figure 6 shows the tip vortex evolution for the straight and the anhydral tip cases. The GT-ENO code shows the formation of the tip vortex in clear detail, and the vortex appears to be well resolved for significant distances downstream of the blade trailing edge. For the anhydral tip, in addition to the tip vortex, a smaller secondary vortex was seen at the location where the blade begins to bend . Figure 7 shows the vortex iso-surface plot for the anhydral tip case. It is seen that this iso-surface preserves its shape, without excessive diffusion for at least 180 degrees of azimuth.

Figure 8 shows the radial variation of the sectional lift and drag coefficients for the anhydral tip case. The comparisons with the HELIX code are not as good here as for the straight tip. The peak lift coefficient near the tip was equal for these two codes. The GT-ENO code predicts that this peak occurs more inboard.

The blade vortex interaction, i.e. the interaction of the tip vortex generated by a blade with the following blade is now studied. Figure 9 shows the vorticity contours for the anhydral case at a typical chordwise location. For reference, the straight blade tip has also been drawn, but the vorticity contours are for the anhydral case. In figure 10, the vorticity contours in the vicinity of the straight blade are shown, with the anhydral tip drawn for reference purposes only. Figures 9 and 10 show that the vortex core for the two blades is at nearly the same geometric location for the two blade tips. In other words, the vortex descent and contraction over a 180 degree azimuth for the two cases are nearly equal. This is confirmed when these two figures are plotted one on top of the other, in figure 11. The two tip vortices are virtually indistinguishable from one another.

CONCLUDING REMARKS

Calculations were carried out for two separate two-bladed rotors in hover, one with a straight tip and the second with an anhydral. The simulations show that the vortices descend and contract by approximately the same amount, if all other parameters such as rotor diameter, tip Mach number and collective pitch are equal. The clearance between the tip vortex and the rotor disk has not increased with the use of the anhydral tip shape, as hoped.

These calculations are preliminary, and must be repeated on a fine grid, for a longer periods of time. Additional one-to-one comparisons with more efficient, "potential flow " methods such as HELIX code must also be carried out. This calibration will allow the designers to use efficient methods such as the HELIX code at low thrust settings, and viscous analyses such as the GT-ENO code at high pitch settings with confidence.

ACKNOWLEDGEMENTS

Financial support for this work provided by the NASA Ames University Consortium office is gratefully acknowledged.

REFERENCES

1. Hariharan, "High Order Simulation of Unsteady Compressible Flows Over Interacting Bodies with Overset grids," Ph. D. Dissertation, Georgia Institute of Technology, August 1995.

2. Ramachandran, K., Tung, C. and Caradonna, F. X., "Rotor Hover Performance Prediction Using a Free-wake Computational Fluid Dynamics Method, " *Journal of Aircraft*, Vol. 26, December 1989, pp. 1105-1110.

3. Ramachandran, K., Moffitt, R. C., Owen, S. J. and Caradonna, F. X., " Hover Performance Prediction using CFD, " 50th Annual AHS Forum, June 1994.

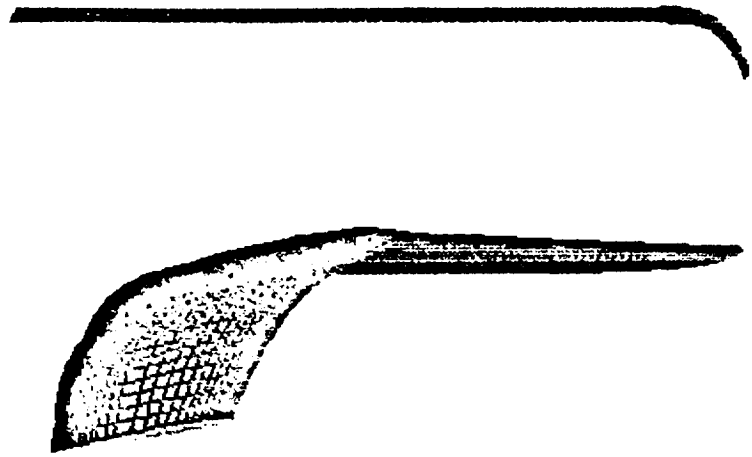

Planform and the H-H grid system

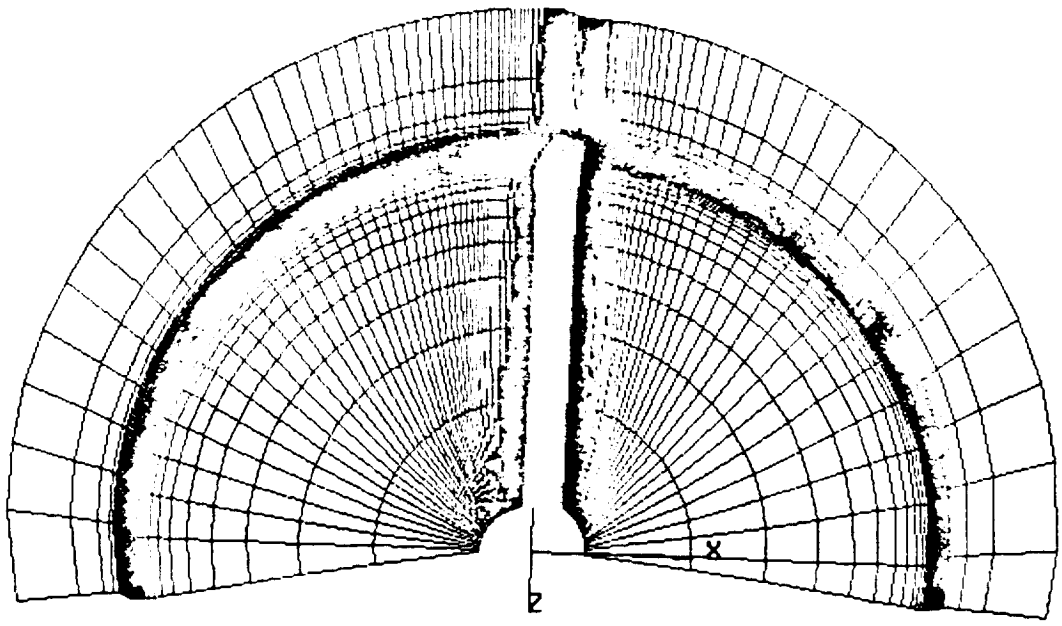

Figure 1. Overview of the Bodyfitted grid

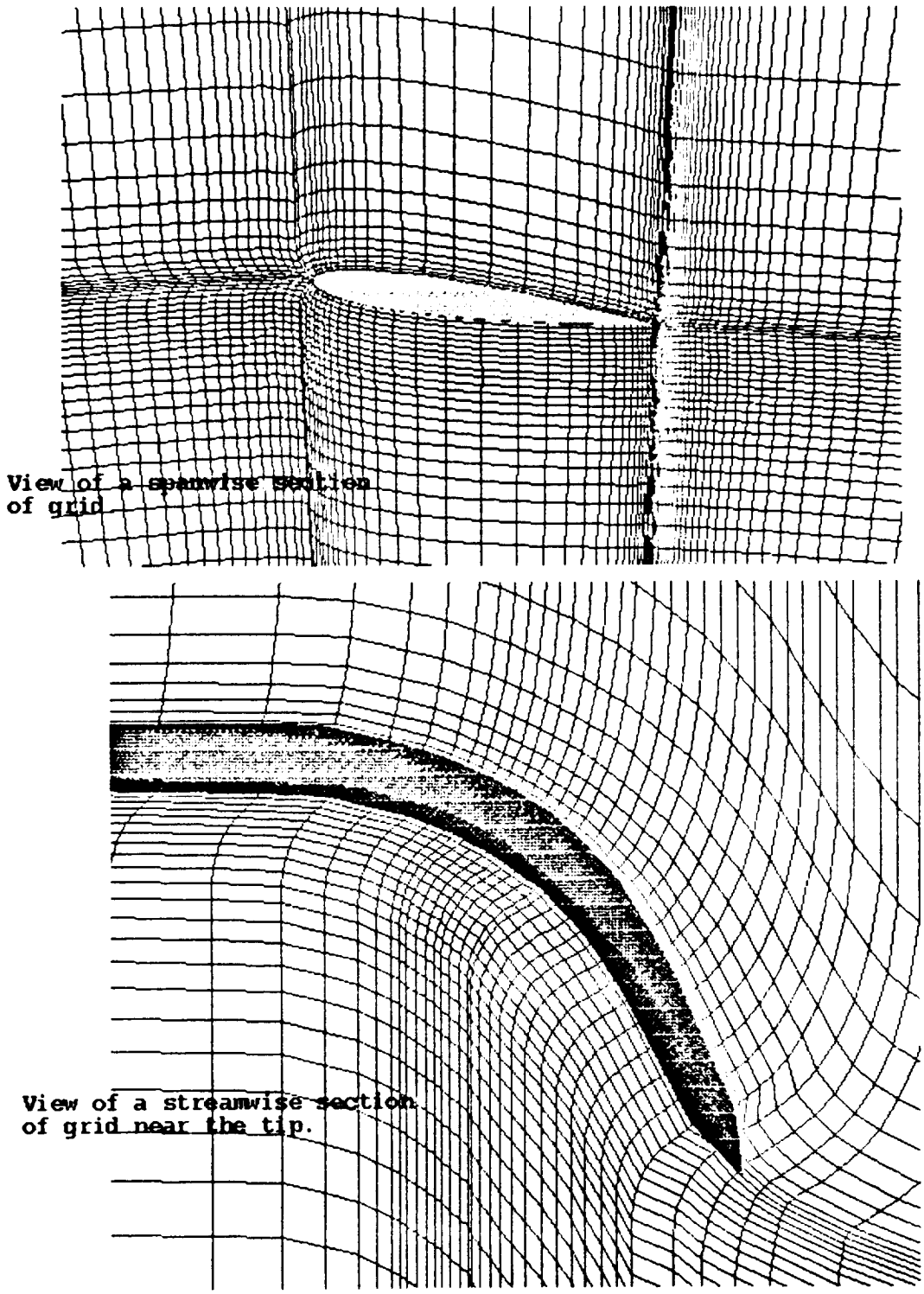

Figure 2. Details of the Body-Fitted Grid in the Vicinity of the Tip

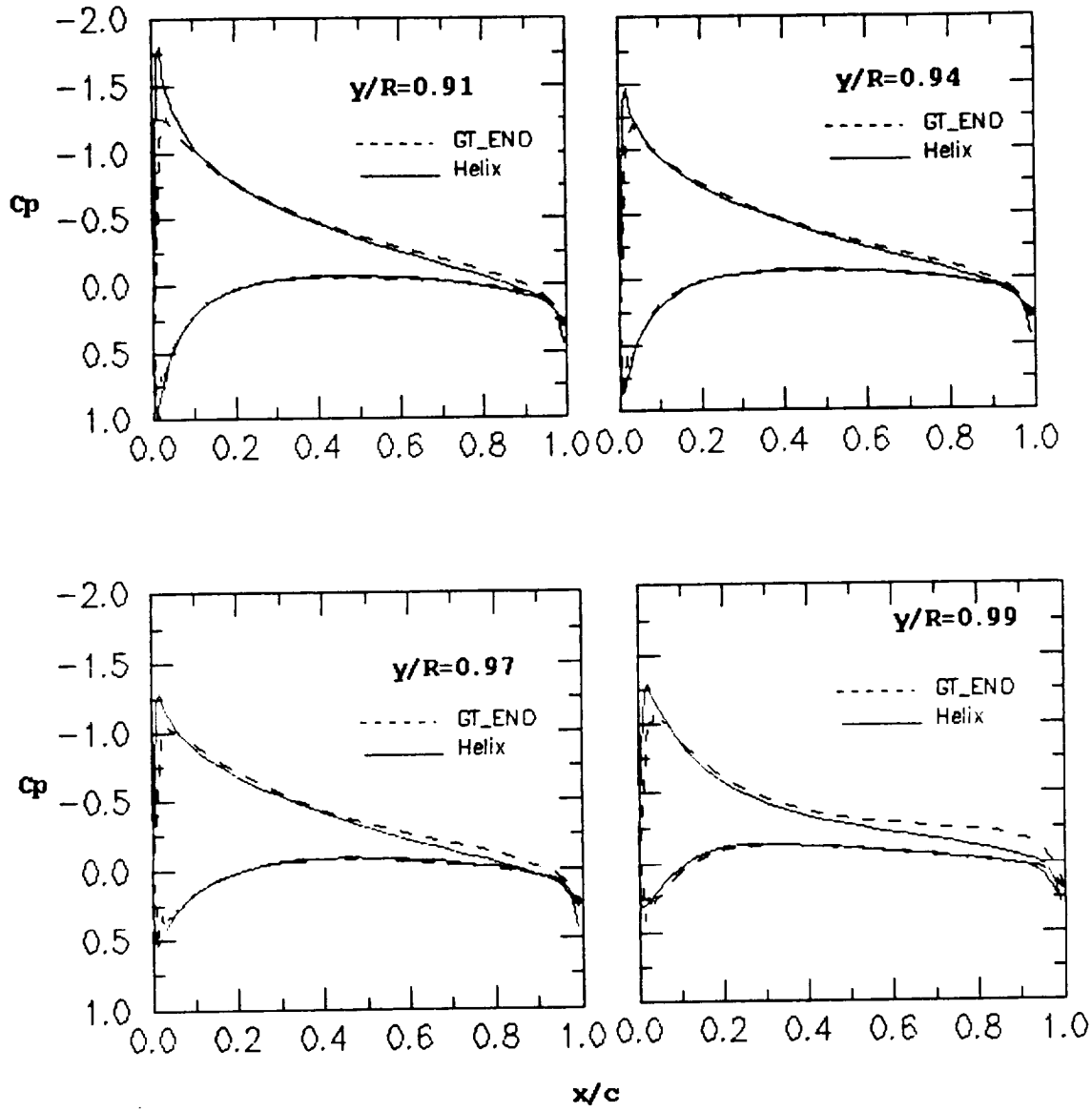

Figure 3. Comparisons between the GT-ENO code and the HELIX Code for the Surface Cp distribution over the Straight Tip

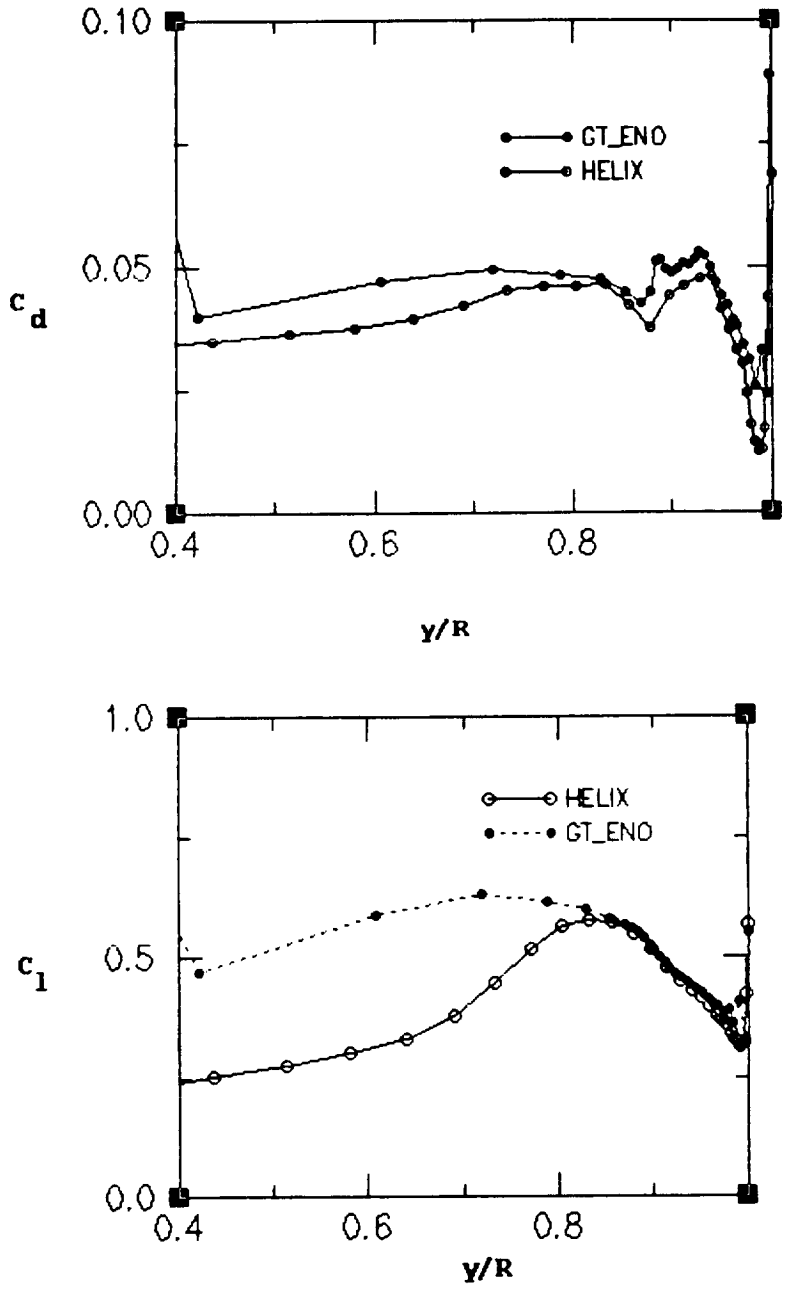

Figure 4. Spanwise Loading over the Straight Tip Predicted by the GT-ENO and HELIX Codes

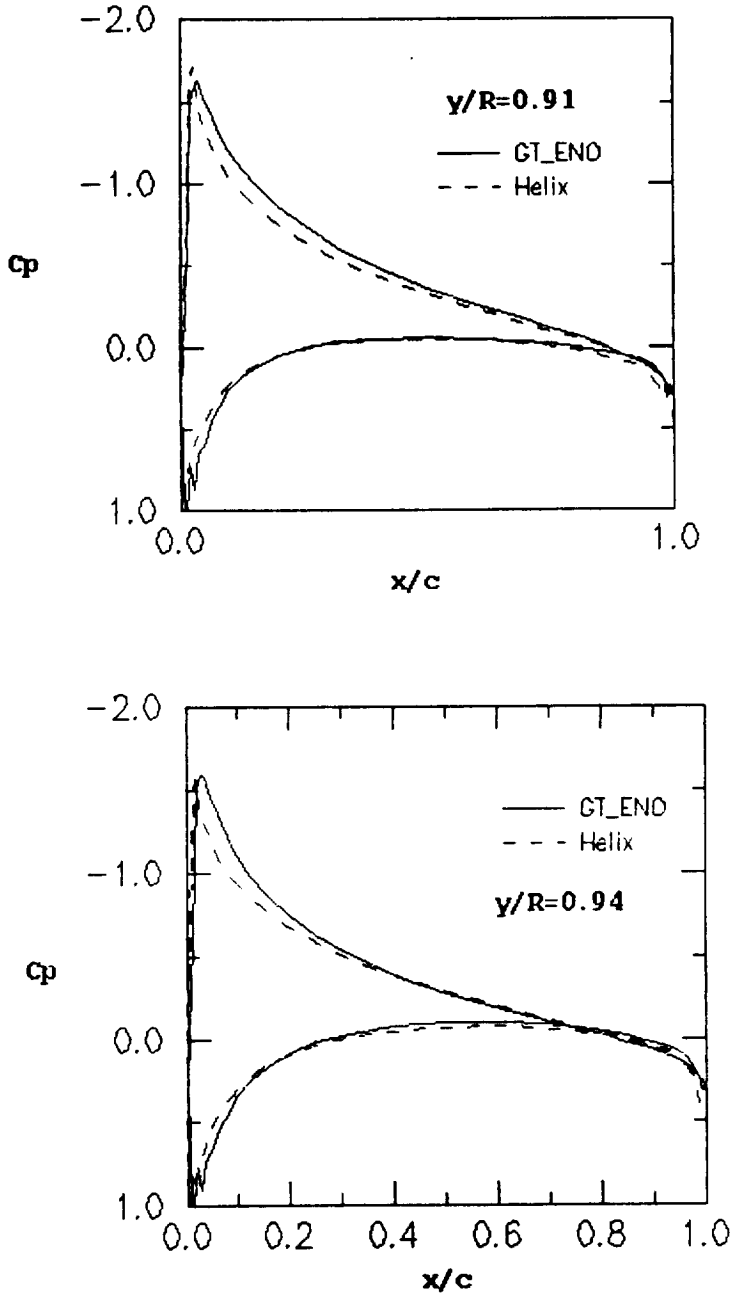

Figure 5. Surface Pressure Distribution over the Anhydral Tip from the GT-ENO and HELIX Codes

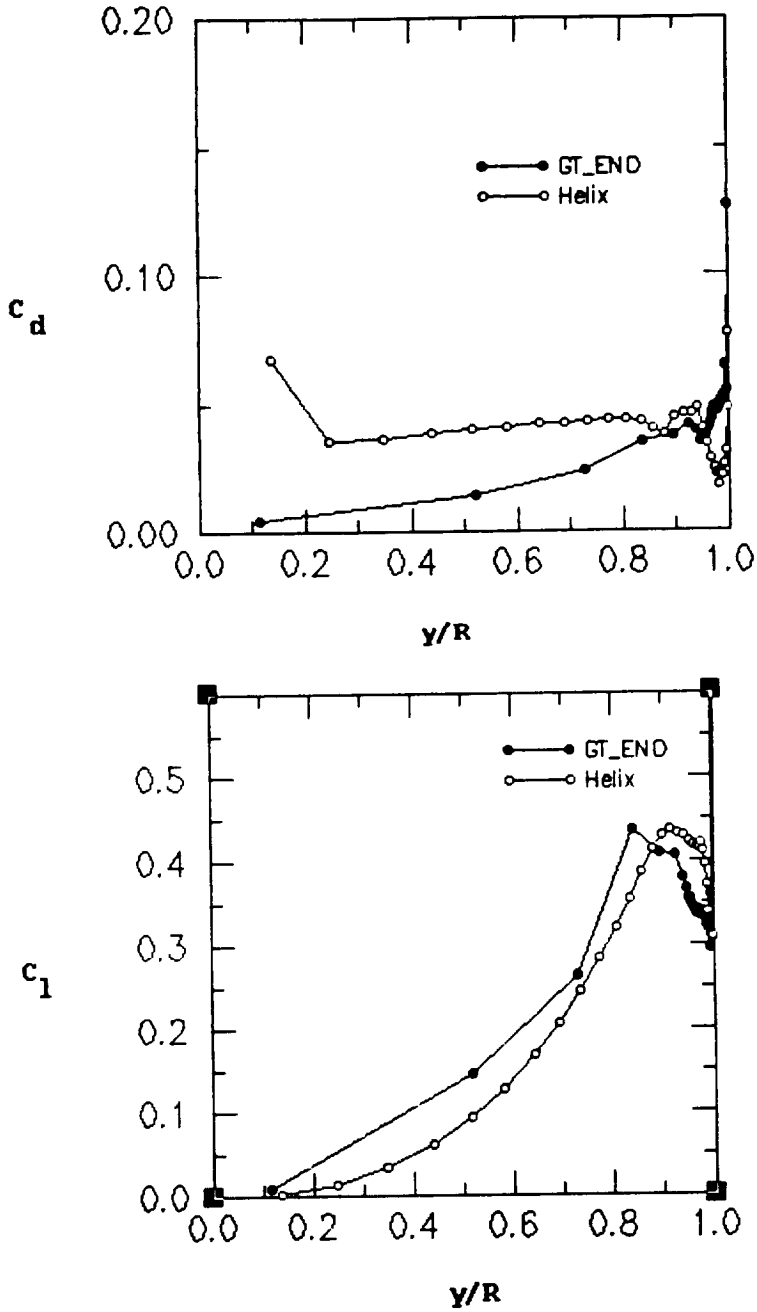

Figure 6. Spanwise Blade Loading over the Anhydral Tip Predicted by the GT-ENO and HELIX Codes

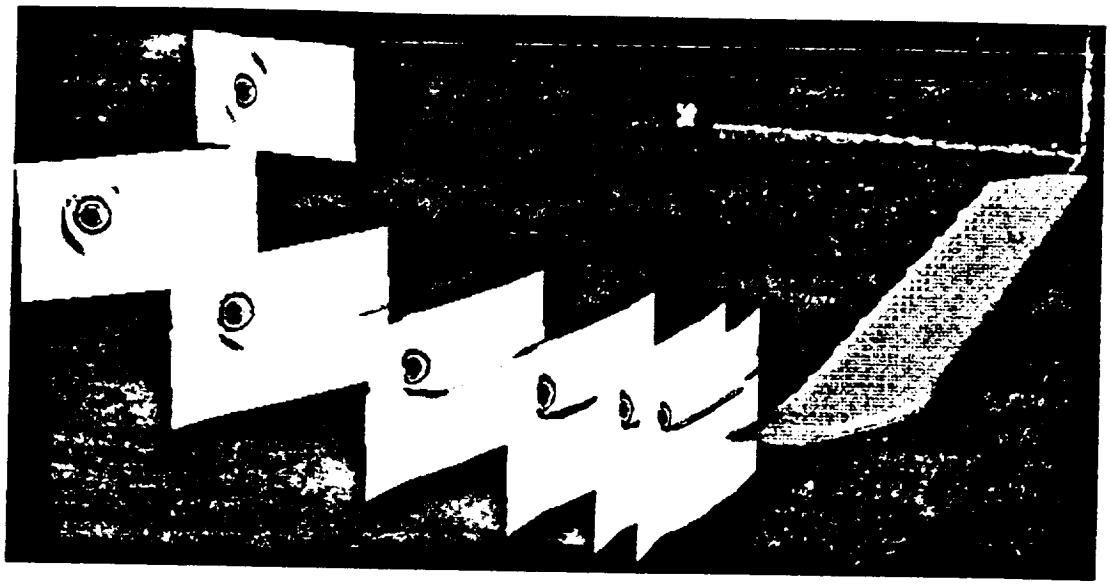

Tip Vortex Evolution: Non-anhedral planform.

Tip Vortex Evolution: Anhedral planform.

Vorticity magnitude contours at various streamwise stations

Figure 7. Comparison of the Tip Vortex Evolution for the Straight and Anhydral Tip

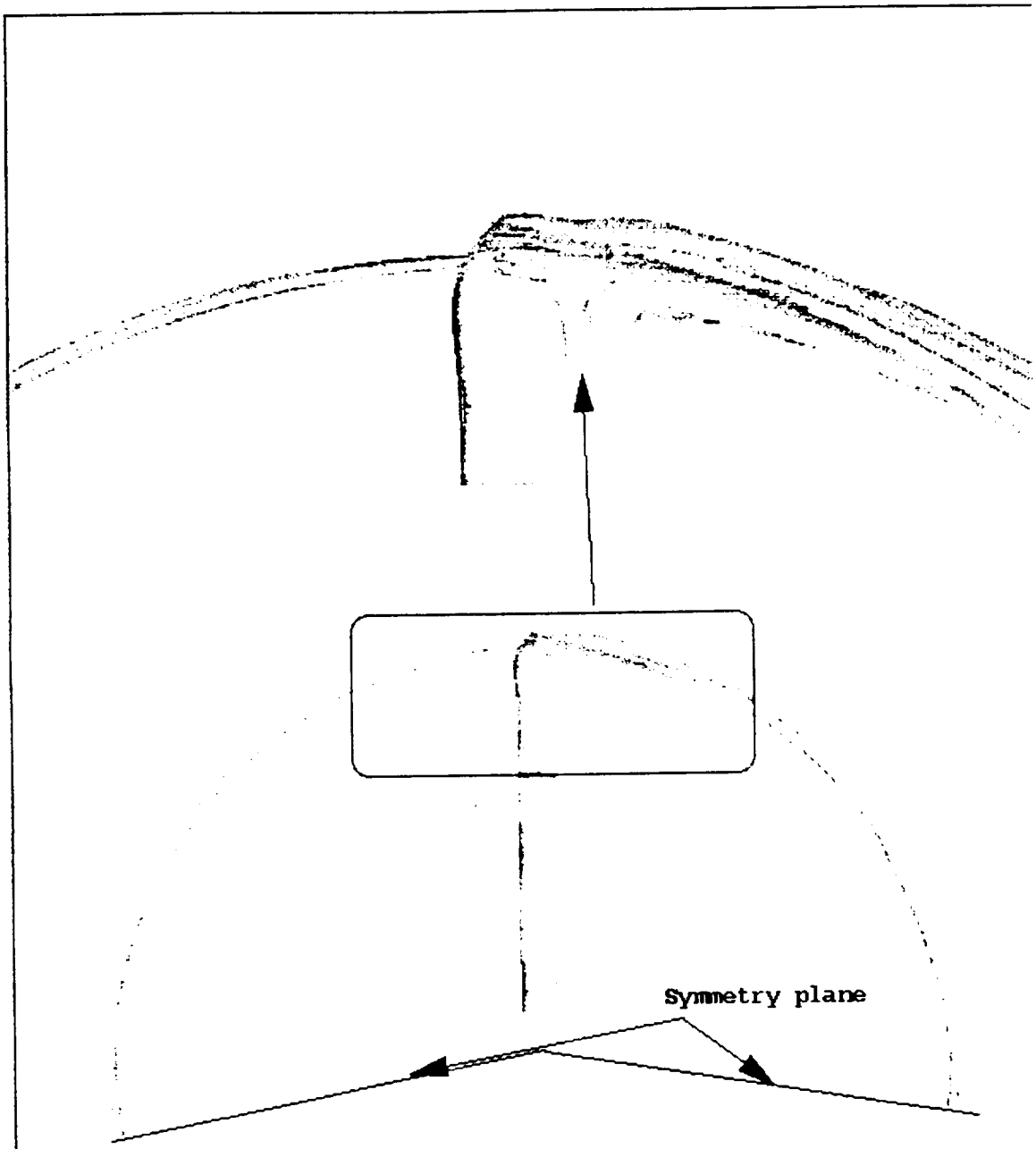

Vorticity iso-surface for the flowfield computed using GT_ENO. Anhedral planform.

Figure 8. Voritcity Iso-surfaces Computed by the GT-ENO code for the Straight and Anhydral Tips

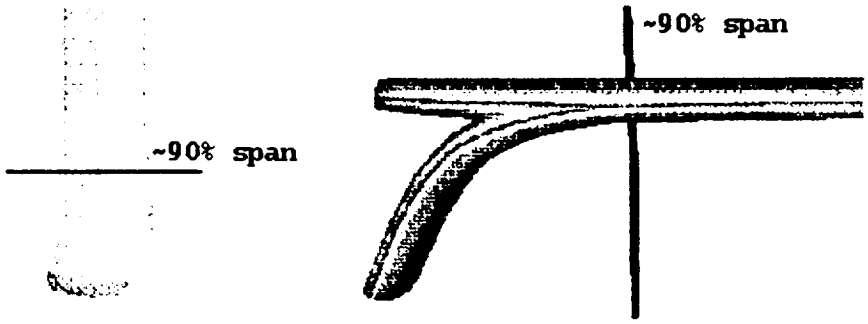

The anhedral and non-anhedral planform surfaces plotted together

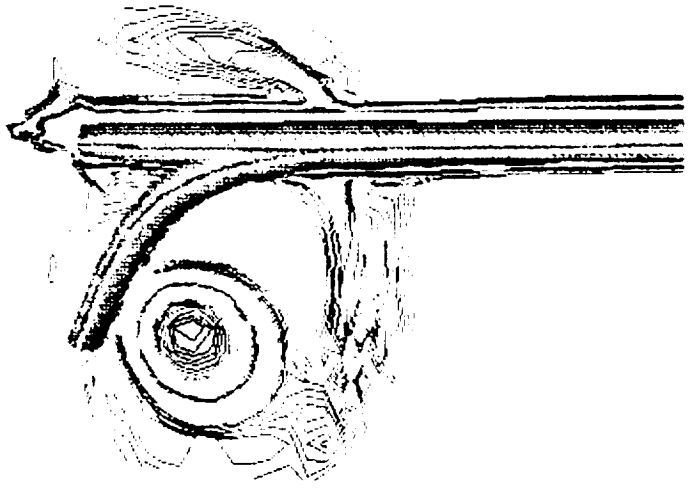

(a) Position of the vortex from the non-anhedral planform
(Vorticity contours computed at a 75% chordwise station, using GT_ENO for the non-anhedral planform)

Figure 9. Position of the Vortex shed from the Previous Blade for the Straight Blade Tip

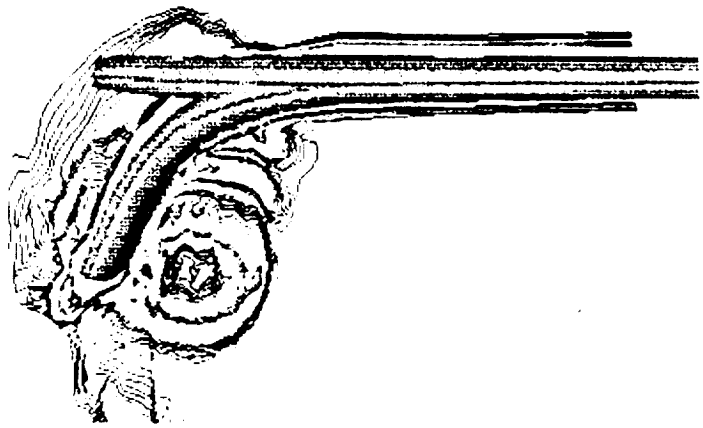

(b) Position of the vortex from the anhedral planform

(Vorticity contours computed at a 75% chordwise station, using GT_ENO for the anhedral planform)

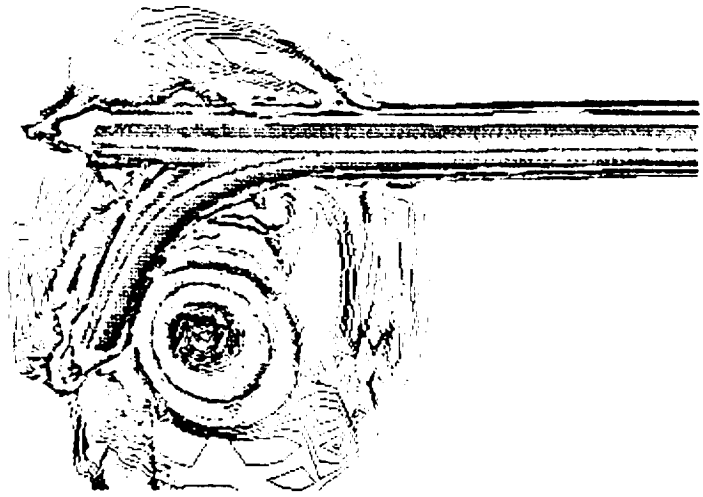

(c) Voriticity contours from the anhedral and non-anhedral computations plotted on top of each other for positional reference.

Figure 10 (Top). Vortex Shed from the Previous Blade for the Anhydral Tip

Figure 11. (Bottom) Tip Vortices for the Straight Blade and Anhydral Blade Superposed on Top of Each Other